

論文の内容の要旨

論文題目 Optical Study of Magnetoelectric Coupling in Antiferromagnetic MnTiO₃

(反強磁性体MnTiO₃における電気磁気結合の光学的研究)

氏 名 佐藤 樹

1. Introduction

Real-space imaging is one of the most powerful techniques to study the magnetic domain pattern and domain-wall dynamics, both of which influence the macroscopic magnetic properties such as magnetization \mathbf{M} and magnetic susceptibility χ . Recently, antiferromagnets with little or no spontaneous magnetization are attracting growing attention by virtue of no stray field and potential high-speed dynamics [1]. However, the absence of spontaneous magnetization makes it difficult to control and visualize antiferromagnetic domain structures [2].

Magnetic domains in antiferromagnets are characterized by the orientation of the staggered magnetization $\mathbf{L} = \mathbf{M}_1 - \mathbf{M}_2$, where \mathbf{M}_i ($i = 1; 2$) is the sublattice magnetization. Magnetoelectric (ME) effect, i.e. electric (magnetic) induction of magnetization (electric polarization \mathbf{P}), offers a clue to control and visualize antiferromagnetic domains. Since the ME coefficient a changes sign under the sign change of \mathbf{L} , the induced \mathbf{P} by external magnetic field \mathbf{H} is opposite between the antiphase antiferromagnetic domains. This feature enables to control \mathbf{L} by the combination of external electric and magnetic fields.

Furthermore, simultaneous breaking of parity-inversion (\mathcal{P}) and time-reversal (\mathcal{T}) symmetries in ME antiferromagnets often induces the directional dichroism of unpolarized light termed magnetochiral dichroism (MCHD) [3]. Such an optical effect associated with the symmetry breaking by the magnetic ordering can be utilized to distinguish antiferromagnetic domains. Imaging studies of the antiferromagnetic domain pattern in combination with external-field control of \mathbf{L} in ME materials would provide insight into antiferromagnetic domain-wall dynamics.

MCHD is described as the asymmetry in the absorption coefficient α between two configurations with respect to the propagation direction \mathbf{k} of light and the magnetic toroidal moment \mathbf{T} , represented

as $\alpha(\mathbf{T} \uparrow \uparrow \mathbf{k}) \neq \alpha(\mathbf{T} \uparrow \downarrow \mathbf{k})$. $\alpha(\mathbf{T} \uparrow \uparrow \mathbf{k})$ and $\alpha(\mathbf{T} \uparrow \downarrow \mathbf{k})$ refer to absorption coefficients when \mathbf{T} is parallel and antiparallel to \mathbf{k} , respectively. \mathbf{T} is proportional to the off-diagonal antisymmetric component in the ME tensor. MCHD has been discovered in chiral materials under a high magnetic field [4] and been investigated in chiral materials with nonzero spontaneous or induced \mathbf{M} . Although above-mentioned correlation between \mathbf{T} and \mathbf{L} enables imaging domain patterns, MCHD for visible light in ME antiferromagnets remains elusive.

MnTiO₃, which crystallizes in the ilmenite structure with the centrosymmetric space group $R\bar{3}$, is known as an ME antiferromagnet with $\mathbf{T} \parallel \mathbf{c}$. Buckled honeycomb layers consisting of Mn²⁺ with $S = 5/2$ and those of nonmagnetic Ti⁴⁺ alternately stack along the c axis. Below the critical temperature $T_N = 65$ K, MnTiO₃ adopts the collinear antiferromagnetic ordering with $\mathbf{L} \parallel \mathbf{c}$ [5]. Two distinct antiferromagnetic states with the c -component of \mathbf{L} , L_c , in opposite directions can form antiphase domains [see Fig. 1(a)]. Magnetic symmetry $\bar{3}'$ allows the linear ME effect represented as

$$\begin{pmatrix} P_{[100]} \\ P_{[120]} \\ P_{[001]} \end{pmatrix} = \begin{pmatrix} a_{\perp} & a_t & 0 \\ -a_t & a_{\perp} & 0 \\ 0 & 0 & a_{\parallel} \end{pmatrix} \begin{pmatrix} H_{[100]} \\ H_{[120]} \\ H_{[001]} \end{pmatrix},$$

Here, the off-diagonal antisymmetric component a_t is associated with the c -component of \mathbf{T} , T^c . From symmetry consideration, the signs of T^c and ME tensor are in one-to-one correspondence with that of L_c [see Fig. 1(a)]. The sign reversal in α between two configurations hence enables MCHD-based imaging of antiferromagnetic domain patterns in MnTiO₃.

2. Results and Discussions

2.1 Magnetochiral dichroism in an antiferromagnet with no magnetization

To verify the MCHD in MnTiO₃, we measured the difference between the spectra of $\alpha(\mathbf{T} \uparrow \uparrow \mathbf{k})$ and $\alpha(\mathbf{T} \uparrow \downarrow \mathbf{k})$. We switch \mathbf{T} with keeping \mathbf{k} fixed. T^c is reversed with the reversal of E_c of ± 2.2 MV/m in $\mu_0 H_c = 6$ T. Figure 1(c) shows the difference spectra $\Delta\alpha d = \alpha d(E_c > 0) - \alpha d(E_c < 0)$ at 55 K and 80 K, where d denotes the sample thickness.

The dip around 2.15 eV at 55 K $< T_N$ in Fig. 1(c) clearly indicates MCHD in MnTiO₃. The absence of $\Delta\alpha d$ at 80 K $> T_N$ shows that antiferromagnetic ordering without \mathcal{P} or \mathcal{T} symmetry is essential for MCHD. Comparing the difference

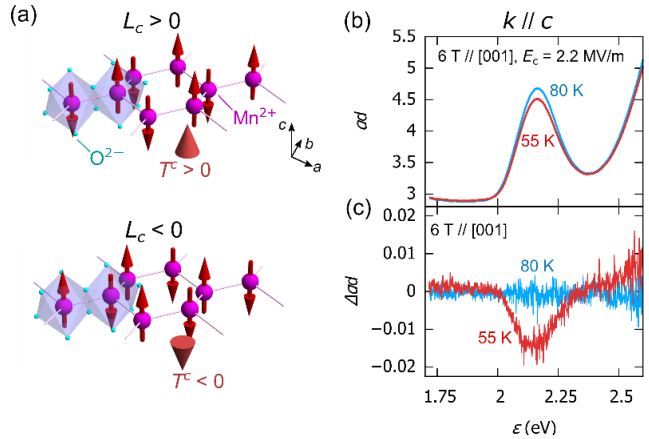


Figure 1: (a) Two distinct antiferromagnetic states of MnTiO₃ with \mathbf{L} in opposite directions. Red arrows represent spins $S = 5/2$ of Mn²⁺. Red cones represent \mathbf{T} . (b) Absorption spectra of MnTiO₃ at 55 K and 80 K in $\mu_0 H_c = 6$ T and $E_c = 2.2$ MV/m. (c) Difference spectra $\Delta\alpha d = \alpha d(E_c > 0) - \alpha d(E_c < 0)$ of MnTiO₃ at 55 K and 80 K.

spectra with the absorption spectra of MnTiO₃ in Fig. 1(b), the dip in Δad corresponds to a peak in ad , which is assigned to an intra-atomic $d-d$ excitation from the ${}^6A_{1g}$ ground state to the ${}^4T_{1g}$ excited state of the octahedrally coordinated Mn²⁺ with d^5 electrons. Combination of staggered ordering of both magnetic moments and chiral distortions of MnO₆ clusters induces MCHD in MnTiO₃.

2.2 Magneto-chiral-imaging of antiferromagnetic domain pattern

The schematic of the optical setup for MCHD-based imaging of antiferromagnetic domain structures in MnTiO₃ is illustrated in Fig. 2(a). Monochromatized light from a halogen lamp was introduced to propagate along the c axis of the crystal. The transmitted light was detected by a charge-coupled detector camera. To reduce the influence of the roughness of the surface of the crystal, difference images were obtained by subtracting reference images without domain patterns.

Figure 2(b) shows a difference image of a MnTiO₃ crystal without any external fields. Prior to the experiment, the crystal was cooled down from 120 K in the absence of external fields. A pronounced domain pattern arises in the circular field of view. The origin of the contrast in Fig. 2(b) is investigated through the temperature dependence of the difference in the transmitted light intensity between brighter and darker areas. The relative difference in brightness is defined as $\Delta I_{AB}/I_{AB} = (I_A - I_B)/(I_A + I_B)$. Here $I_{A(B)}$ is the average intensity of the area A (B) computed as $I_{A(B)} = \int_{A(B)} d\mathbf{r} I(\mathbf{r}) / \int_{A(B)} d\mathbf{r}$. $I(\mathbf{r})$ denotes the transmitted light intensity at pixel position \mathbf{r} in the original picture. $\int_{A(B)} d\mathbf{r}$ denotes the integral over a square labeled A (B) in Fig. 2(b). The $\Delta I_{AB}/I_{AB}$ increases as the sample is cooled below $T_N = 65$ K, as shown in Fig. 2(c). Temperature dependence of the magnetic susceptibility χ along the c axis is also shown in Fig. 2(d). Figures 2(c) and (d) clearly evidence the magnetic origin of the contrast in Fig. 2(b). The magnetically induced change in $\Delta I_{AB}/I_{AB}$ at 55 K in Fig. 2(c) is as large as 1% , corresponding to the magnitude of MCHD at 2.16 eV in MnTiO₃ [see Fig. 1(c)]

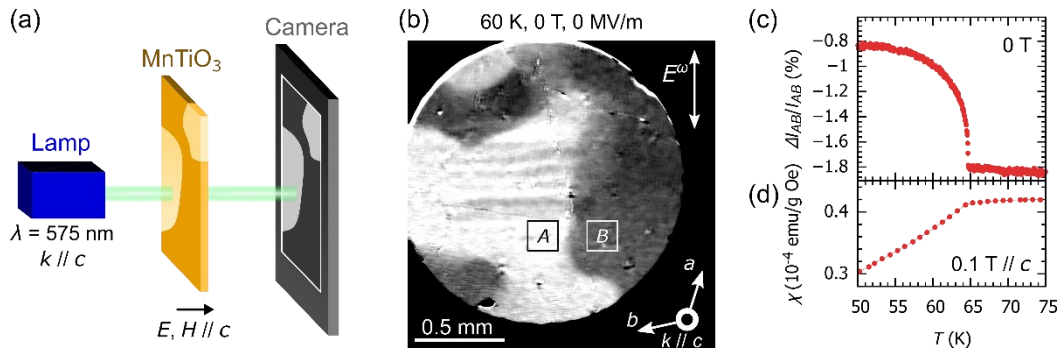


Figure 2: (a) Schematic of antiferromagnetic domain imaging based on magneto-chiral dichroism in MnTiO₃. (b) Difference image at 60.0 K. An image at 65.0 K is used as the reference. (c) Temperature dependence of the relative difference $\Delta I_{AB}/I_{AB}$ in the integrated intensity between square regions A and B indicated in (b) at 0 T. (d) Temperature dependence of the magnetic susceptibility χ along the c axis.

2.3 Imaging study of magnetoelectric domain-reversal dynamics

We investigate the domain wall dynamics in the antiferromagnetic domain reversal by repetitive imaging of domain patterns. As shown in Fig. 3(a), each cycle of the measurement in $\mu_0 H_c = 0.1$ T consists of three parts: (i) First, a negative electric field $E_c = -7.9$ MV/m is applied for poling. (ii) Second, a positive pulsed electric field of an amplitude $E_c = 7.9$ MV/m is applied for time Δt . The electric field is then turned off. (iii) Finally, the domain image is recorded at zero electric field.

Since the driving force for domain

walls is zero in the absence of E_c , a domain pattern exactly at time Δt after abrupt switching of E_c from -7.9 MV/m to 7.9 MV/m is recorded in the third step. By collecting several images at various Δt , the overall picture in the inversion process can be grasped.

Figures 3(b)-(e) show difference images at several values of Δt . The darker antiferromagnetic domain continuously expands by increasing Δt . The millisecond dynamics in the antiferromagnetic domain-wall motion driven by DC electric and magnetic fields in magnetoelectric MnTiO₃ is clearly captured. Detailed investigation of the domain-wall velocity v_{DW} at various E_c and temperatures suggests a divergent enhancement in domain-wall mobility with approaching T_N .

3. Summary

In this thesis, we investigate MCHD in MnTiO₃. We observed the MCHD in an antiferromagnet MnTiO₃, which indicates that the staggered ordering of magnetic moments in antiferromagnets in the presence of antiferrochiral ordering can be a source of MCHD even without any magnetization. Observed MCHD enabled us to visualize antiferromagnetic domain patterns. The millisecond dynamics of the antiferromagnetic domain wall driven by DC electric and magnetic fields is clearly captured. This work demonstrates that MCHD-based imaging technique can be applied to the studies of magnetic domain-wall dynamics in ME antiferromagnets.

References

- [1] V. Baltz et al., Rev. Mod. Phys. **90**, 015005 (2018). [2] S.-W. Cheong et al., npj Quantum Mater. **5**, 1 (2020). [3] L. Barron and J. Vrbancich, Mol. Phys. **51**, 715 (1984). [4] G. L. J. A. Rikken and E. Raupach, PRE **58**, 5081 (1998). [5] G. Shirane et al., JPSJ **14**, 1352 (1959).

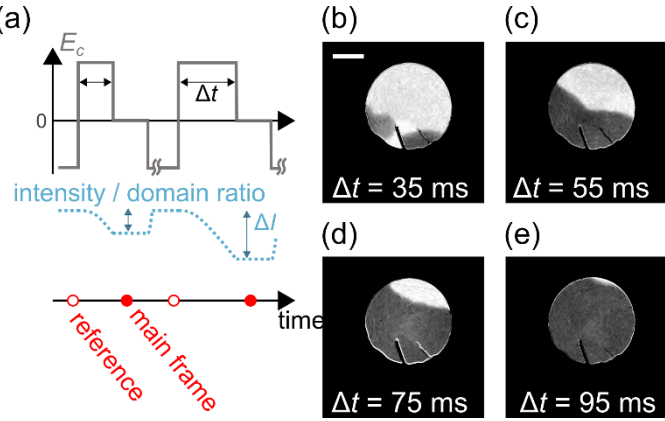


Figure 3: (a) Timing scheme of the experiment. Reference images were recorded in every poling process. All the measurements were performed in the presence of $\mu_0 H_c = 0.1$ T. (b-e) Difference c -plane images recorded at several values of Δt . The white bar in (b) corresponds to 0.5 mm.